Stereoselective Metabolism of Fenoxaprop-Ethyl and Its Chiral Metabolite Fenoxaprop in Rabbits

YANFENG ZHANG,[1] XUEFENG LI,[2] ZHIGANG SHEN,[2] XINYUAN XU,[2] PING ZHANG,[2] PENG WANG,[2]* AND ZHIQIANG ZHOU[2]*

[1]*Research Center for Eco-Environmental Sciences, Chinese Academy of Sciences, Beijing, China*
[2]*Department of Applied Chemistry, China Agricultural University, Beijing, China*

ABSTRACT The stereoselective metabolism of the enantiomers of fenoxaprop-ethyl (FE) and its primary chiral metabolite fenoxaprop (FA) in rabbits in vivo and in vitro was studied based on a validated chiral high-performance liquid chromatography method. The information of in vivo metabolism was obtained by intravenous administration of racemic FE, racemic FA, and optically pure (−)-(*S*)-FE and (+)-(*R*)-FE separately. The results showed that FE degraded very fast to the metabolite FA, which was then metabolized in a stereoselective way in vivo: (−)-(*S*)-FA degraded faster in plasma, heart, lung, liver, kidney, and bile than its antipode. Moreover, a conversion of (−)-(*S*)-FA to (+)-(*R*)-FA in plasma was found after injection of optically pure (−)-(*S*)- and (+)-(*R*)-FE separately. Either enantiomers were not detected in brain, spleen, muscle, and fat. Plasma concentration–time curves were best described by an open three-compartment model, and the toxicokinetic parameters of the two enantiomers were significantly different. Different metabolism behaviors were observed in the degradations of FE and FA in the plasma and liver microsomes in vitro, which were helpful for understanding the stereoselective mechanism. This work suggested the stereoselective behaviors of chiral pollutants, and their chiral metabolites in environment should be taken into account for an accurate risk assessment. *Chirality 23:897–903, 2011.*

KEY WORDS: stereoselectivity; chiral analysis; fenoxaprop-ethyl; fenoxaprop; in vivo; in vitro

INTRODUCTION

Fenoxaprop-ethyl (FE, Fig. 1), (±)-ethyl 2-[4-[(6-chloro-2-benzoxazolyl)oxy]phenoxy]propanoate, a selective aryloxyphenoxypropionate herbicide, is registered for postemergence control of various grass weeds in dicotyledonous crops as well as in grains.[1] FE is not persistent in the environment and easily undergoes ester cleavage to its corresponding acid fenoxaprop (FA, Fig. 1), 2-[4-(6-chloro-2-benzoxazolyloxy) phenoxy] propionic acid, which possesses herbicidal activity. FE (or FA) has an asymmetrically substituted C-atom and thus consists of a pair of enantiomers that are (−)-(*S*) and (+)-(*R*),[2] but the herbicidal activity originates from the (+)-(*R*)-enantiomer.

Stereoselective metabolism of chiral pesticides has been observed in various animals in vivo and in vitro. Yang et al.[3] demonstrated that mice and quail have different enantioselective biotransformation of α-Hexachlorocyclohexane (α-HCH), and enantiomer fraction (EF) trends in brain tissues of both animals were quite different from those in other tissues. Wang et al.[4] reported that the degradation of the (+)-theta-cypermethrin was much faster than that of its antipode in plasma, heart, liver, kidney, and fat after i.v. administration of racemic TCYM in rats. Zhu et al.[5] elaborated that the in vivo degradation rate of tebuconazole enantiomers was different. Warner et al. demonstrated that chiral polychlorinated biphenyls were biotransformed enantioselectively by mammalian cytochrome P-450 isozymes to form hydroxylated metabolites in vitro. Such stereoselective degradation in organisms has mainly been attributed to uptake, distribution, metabolism, and excretion, but other biological processes, including selective protein binding and tissue transport, can also influence enantiomer compositions in biota.[6–11]

This study was conducted to evaluate the stereoselectivity of FE and FA in rabbit. First, this research was conducted to get the features of the FE and FA enantiomers in rabbit plasma and tissues after in vivo exposure and obtain a better understanding of the biological fate of each enantiomer in rabbit. Second, the behavior of FE and FA in plasma and liver microsomes from rabbit was conducted to assess the in vitro stereoselective metabolism of FE and FA. All the information may be used in construction of a physiologically based toxicokinetic model for FE and FA in the adult male rabbit and may have some implication for the environmental and ecological risks assessment for chiral pesticides.

MATERIALS AND METHODS

Chemicals and Reagents

Racemic fenoxaprop-ethyl (*rac*-FE, 98.0%) and (+)-(*R*)-fenoxaprop-ethyl (*R*-FE, 98.0%) were kindly provided by Institute for Control of Agrichemicals, Ministry of Agriculture of China. Racemic fenoxaprop (*rac*-FA, 97.5%) was obtained from the hydrolysis of their corresponding parent compounds. (−)-(*S*)-Fenoxaprop-ethyl (*S*-FE, 99.0%) was collected manually on an Agilent high-performance liquid chromatography (HPLC) with a chiral column (250 mm × 4.6 mm (i.d.)). β-Nicotinamide adenine dinucleotide phosphate (NADPH) was purchased from Sigma-Aldrich (St Louis, MO). Hexane, 2-propanol (HPLC grade), and trifluoroacetic acid (TFA) were from Yili Fine Chemicals (Beijing, China). Water

Contract grant sponsor: National Natural Science Foundation of China; Contract grant number: 20707038.
*Correspondence to: Peng Wang, China Agricultural University, Beijing, China. E-mail; wangpeng@cau.edu.cn or Zhiqiang Zhou, China Agricultural University, Beijing, China. E-mail: zqzhou@cau.edu.cn
Received for publication 7 December 2010; Accepted 29 June 2011
DOI: 10.1002/chir.21009
Published online 20 September 2011 in Wiley Online Library (wileyonlinelibrary.com).

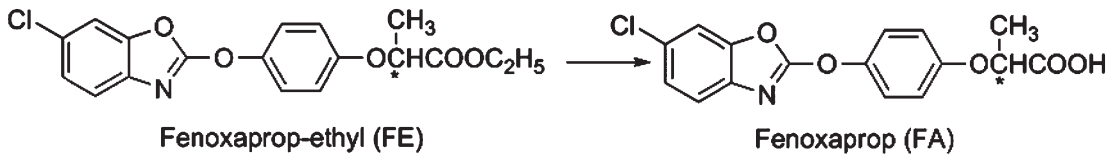

Fig. 1. Chemical structures of fenoxaprop-ethyl and its primary metabolite fenoxaprop. Chiral center is denoted by an asterisk (*).

was purified by a Milli-Q system. All other chemicals and solvents were of analytical grade and purchased from commercial sources.

The procedure of preparation of rabbit hepatic microsomes from rabbits (Japanese white rabbit, male, Approximately 2 kg, provided by the Experimental Animal Research Institute of China Agriculture University) followed the method of Zhang et al.[12] and the microsomes were immediately stored at −80°C. Hepatic microsomal activity was determined according to the method of Bradford with BSA as the standard.

Degradation Kinetic and Toxicokinetic Assays

Drug administration and sample collection. Male Japanese white rabbits (~2 kg) were fasted for 12 h before the experiment. Racemic FE or FA was dissolved in alcohol (50%, w/v), diluted to final concentrations by normal saline, and then administered at 30 mg/kg body weight by intravenous (i.v.) injection in the ear vein. Blood samples were collected from the heart of treated rabbits into heparinized tubes at 0.5, 1, 1.5, 2, 3, 4, 8, and 12 h after exposure; each data point is the mean of six replicates. Blood was centrifuged at 4000 rpm for 10 min, and plasma was transferred into a new test tube. After all blood samples collection, the rabbits were killed at 12 h after being anesthetized. The heart, kidney, liver, lung, fat, muscle, spleen, bile, and brain samples were collected from each subject. Plasma and tissue samples were stored at −20°C for further treatment. To determine the chiral conversion of the two FE enantiomers in the rabbit, (−)-(*S*)- and (+)-(*R*)-FE were also administered separately at 15 mg/kg body weight in the same manner as mentioned above.

Extraction procedure. After being thawed, 1 ml of the rabbit plasma or 1 g of homogenized tissue matrix was transferred into a 15-ml polypropylene centrifuge tube, acidified with 100 μl of 1 M HCl, and added with 5 ml of ethyl acetate.[13] After vortex for 5 min and centrifugation at 4000 rpm for 5 min, the clear organic supernatant was decanted into a test tube. The extraction was repeated with another 5 ml of ethyl acetate. The organic phase was combined and evaporated to dryness under a stream of nitrogen at 40°C. To get rid of fat, the residue was dissolved in 1 ml of acetonitrile and partitioned thrice with 2 ml of *n*-hexane, and then the acetonitrile phase was evaporated to dryness under a stream of nitrogen. The residue was reconstituted in 200 μl of 2-propanol and passed through a 0.22-μm syringe filter. A 20-μl aliquot was injected into the HPLC.

Data analysis. EFs were used to denote stereoselectivity, defined by Eq. 1.

$$\mathrm{EF} = \text{Peak areas of the}\frac{(-)}{[(-)+(+)]}, \tag{1}$$

where (−) and (+) are the concentrations of the first eluted (−)-(*S*)-enantiomer and the second eluted (+)-(*R*)-enantiomer. A racemic standard had EF of 0.5, whereas preferential degradation of one of the enantiomers made EF under or over 0.5. Statistical differences between treatments ($P < 0.05$) were determined using a paired *t*-test.

Individual toxicokinetic parameters of FE and FA enantiomers were determined using standard compartmental analysis methods and calculated with the Drug and Statistics software (Section of Quantitative Pharmacology, Chinese Pharmacological Society).

In Vitro Incubation Procedure

Substrate-depletion assays in plasma. The degradations of *rac*-FE, (−)-(*S*)-FE, (+)-(*R*)-FE, and *rac*-FA in rabbit plasma in vitro were performed to investigate the stereoselectivity and the chiral conversion of the enantiomers. Plasma was obtained by centrifugating the blood that was collected from the untreated rabbits at 4000 rpm for 10 min at 4°C. A 10% (v/v) plasma solution was prepared (diluted by Tris-HCl buffer, pH 7.4) and preincubated at 37°C for 5 min, and then the individual substrate (*rac*-FE, (−)-(*S*)-FE, (+)-(*R*)-FE, and *rac*-FA) prepared in alcohol was added into each 1-ml plasma incubation forming a final concentration of 30 μM and incubated at 37°C. Samples were collected at 0, 5, 15, 30, and 60 min, and 5 ml of ice-cold ethyl acetate was added immediately to terminate the enzyme–substrate reaction. One set of similar incubations without substrate was served as control. The extraction procedure was the same as mentioned above.

Substrate-depletion assays in microsomes. The stereoselective degradations of *rac*-FE, (−)-(*S*)-FE, (+)-(*R*)-FE, and *rac*-FA in rabbit liver microsomes in vitro were also conducted. Each incubation (1.0 mg protein per milliliter, adjusted by Tris-HCl buffer of pH 7.4) was added with the substrate in alcohol to a concentration of 30 μM and preincubated at 37°C for 5 min. The reaction was regenerated with 100 μl of NADPH to a final concentration of 1.0 mM (final total reaction volume 1.0 ml). Samples were taken out after incubation at 37°C for 0, 5, 15, 30, and 60 min, respectively, and 5 ml of ice-cold ethyl acetate was added to terminate the reaction. One set of similar incubations without substrate was served as control. The extraction procedure was the same as mentioned above.

Enzyme kinetic experiments in liver microsomes. The stereoselective disappearance of *rac*-FE or *rac*-FA in the rabbit liver microsomes in a series of concentrations 5, 15, 30, 60, 120, 240, and 300 μM was conducted to assess the relative contributions of enzymes such as esterases and CYP450s responsible for FE and FA metabolism based on the relationship of stereoselective disappearance and substrate concentrations.[14] The incubating time was 30 min, and other procedures were the same as those in substrate-depletion assays in microsomes.

Data analysis. Michaelis–Menten rate constants for FE and FA disappearance were calculated using linear and nonlinear regression as applicable with Origin 7.5 software yielding the maximum velocity (V_{max}) and affinity constant (K_m), using the following Eq. 2:

$$V = \frac{V_{\max} \times S}{K_m + S}, \tag{2}$$

where V, S, V_{max}, and K_m represent the rate of metabolism, substrate concentration, maximum rate of metabolism, and Michaelis constant, respectively. The metabolic efficiency was estimated by calculating intrinsic clearance (CL_{int}) by the following Eq. 3:

$$\mathrm{CL}_{\mathrm{int}} = \frac{V_{\max}}{K_m}. \tag{3}$$

Apparatus and Chromatographic Conditions

Analytes were quantified using an Agilent 1200 series HPLC system (Agilent Technology) equipped with a G1322A degasser, a G1311A quat pump, a G1329A ALS, a G1314B VWD, and Agilent Chemstation software.

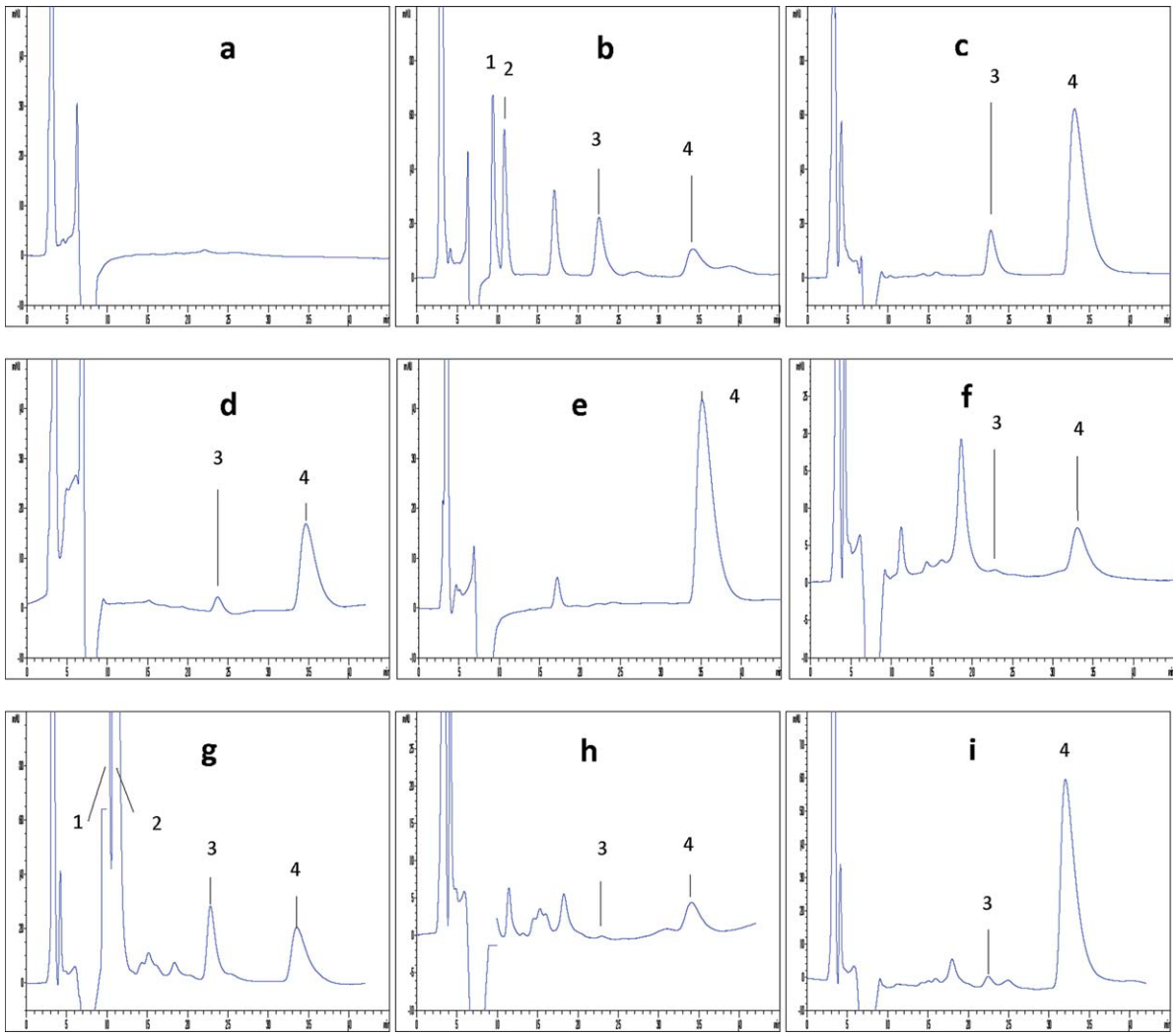

Fig. 2. Representative HPLC chromatograms of plasma and tissues. (**a**) Untreated rabbit plasma; (**b**) untreated plasma spiked with *rac*-FE (10.0 μg/ml) and *rac*-FA (10.0 μg/ml); (**c**) plasma at 0.5 h after i.v. treatment with *rac*-FE at 30 mg/kg body weight; (**d**) plasma at 0.5 h after i.v. treatment with (−)-(*S*)-FE at 15 mg/kg body weight; (**e**) plasma at 0.5 h after i.v. treatment with (+)-(*R*)-FE at 15 mg/kg body weight; (**f**) heart, (**g**) lung, (**h**) liver, (**i**) kidney, and tissue samples collected from a rabbit at 12 h after i.v. treatment with *rac*-FE at 30 mg/kg body weight. Peaks: 1, (−)-(*S*)-FE; 2, (+)-(*R*)-FE; 3, (−)-(*S*)-FA; 4, (+)-(*R*)-FA. [Color figure can be viewed in the online issue, which is available at wileyonlinelibrary.com.]

Enantiomer analysis was performed on an amylose-tri-(3,5-dimethylphenylcarbamate)-based column (250 mm × 4.6 mm (i.d.), provided by the Department of Applied Chemistry, China Agricultural University, Beijing). The chromatographic separation was conducted at 20°C and monitored at 230 nm with the mobile phase containing *n*-hexane–isopropanol–trifluoroacetic acid (95:5:0.1, v/v/v) at a flow rate of 1.0 ml/min.

Method Validation

Blank plasma was spiked with *rac*-FE and *rac*-FA working standard solutions to generate calibration samples ranging from 0.10 to 200μg/ml for the single enantiomer. Calibration samples were prepared as described earlier. Calibration curves were generated by plotting the concentration of each enantiomer in the spiked samples versus the peak area of each enantiomer. The within-day precision was determined in six replicates at concentrations of 1.0, 10.0, and 50.0 μg/ml on the same day, whereas the inter-day precision was evaluated in six replicates at the aforementioned concentrations on 6 different days. The standard deviation (SD) and the relative standard deviation (RSD = SD/mean) were calculated over the entire calibration range. The recoveries were estimated by the peak area ratio of the extracted analytes with an equivalent amount of the standard solution in pure solvents. The limit of detection (LOD) was considered to be the concentration that produced a signal-to-noise (S/N) ratio of 3. The limit of quantification (LOQ) was defined as the lowest concentration in the calibration curve with acceptable precision and accuracy.

RESULTS AND DISSCUSSION

Method Validation

The two pairs of enantiomers: (−)-(*S*)-FE, (+)-(*R*)-FE, (−)-(*S*)-FA, and (+)-(*R*)-FA, were baseline separated under the optimized condition shown in Figure 2b. Linear calibration curves were obtained over the concentration range of 0.10–200 μg/ml for (−)-(*S*)-FE ($y = 220.92x - 41.72$, $R^2 = 0.998$), (+)-(*R*)-FE ($y = 214.03x - 43.18$, $R^2 = 0.998$), (−)-(*S*)-FA ($y = 232.21x - 93.39$, $R^2 = 0.992$), and (+)-(*R*)-FA ($y = 223.21x - 95.14$, $R^2 = 0.993$). The accuracy of the assay for each enantiomer ranged from 3 to 16% (SD) and precision from 3 to 11% (RSD). Recoveries of each enantiomer fortified at 1.0, 5.0, and 50.0 μg/ml ranged from 88% ± 3% to 108% ± 8%. The LOD and LOQ in plasma were 0.03 and 0.1 μg/ml, respectively. The data showed that the method was satisfying.

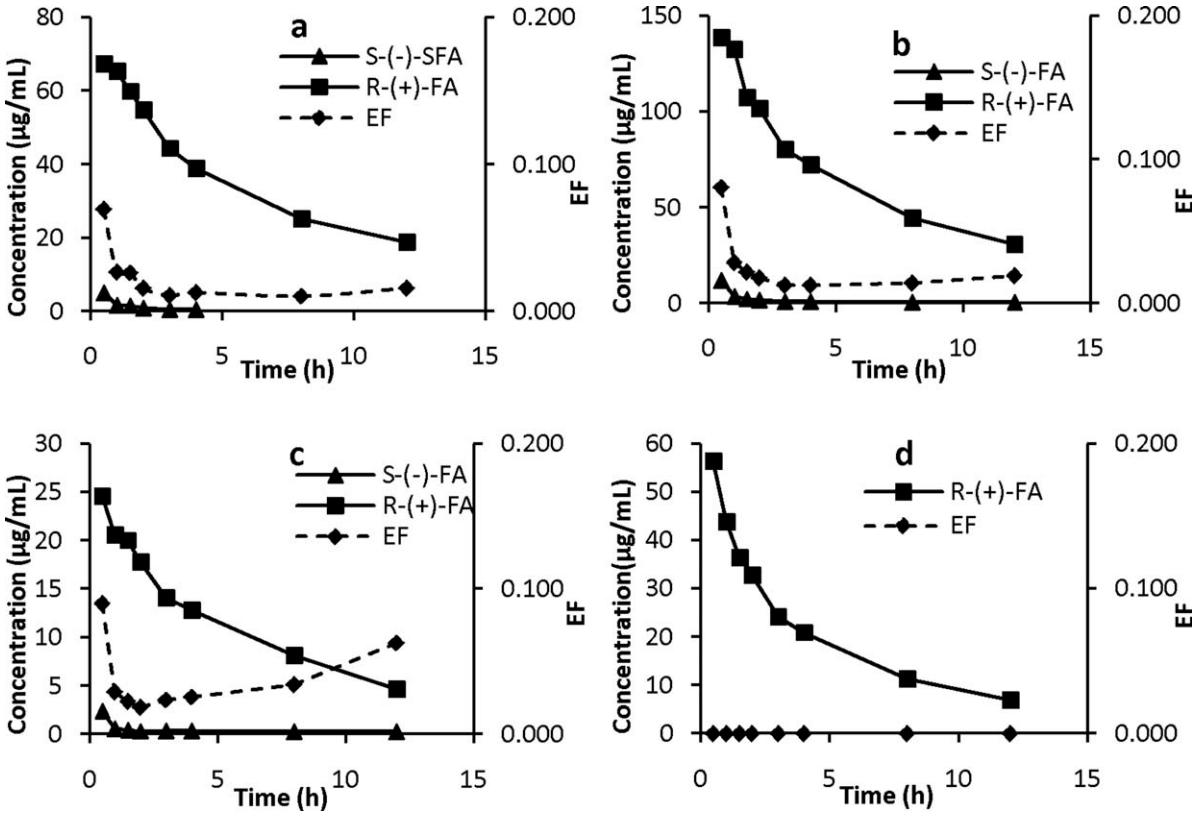

Fig. 3. Plasma concentration–time curves and EFs of FA enantiomers in rabbit following (**a**) *rac*-FE administration at 30 mg/kg body weight; (**b**) *rac*-FA administration at 30 mg/kg body weight; (**c**) (−)-(*S*)-FE administration at 15 mg/kg body weight; and (**d**) (+)-(*R*)-FE administration at 15 mg/kg body weight.

Degradation Kinetic and Toxicokinetic Analysis in Plasma

Racemic parent compound FE was not detected in rabbit plasma after administration of *rac*-FE in 30 mg/kg body weight, which indicated that *rac*-FE was hydrolyzed rapidly to its carboxylated acid FA by esterase. The concentration of produced (+)-(*R*)-FA was much higher than its antipode even in the first time point, and the primary metabolite FA underwent further degradation. The plasma concentration–time curves of (−)-(*S*)- and (+)-(*R*)-FA are shown in Figure 3a, and the degradations followed first-order kinetics. (−)-(*S*)-FA was preferentially degradated (Fig. 2c), and it was not detected at the 12th hour, but (+)-(*R*)-FA still showed a high level of 18.92 mg/kg. The $T_{1/2}$ of (−)-(*S*)-FA and (+)-(*R*)-FA was 1.10 and 6.30 h, respectively. The EFs decreased gradually far from 0.5 showing a prominent enantioselective residue of *R*-enantiomer.

Plasma concentration–time curves of (−)-(*S*)- and (+)-(*R*)-FA after i.v. administration of 30 mg/kg of *rac*-FA are shown in Figure 3b. The degradations also followed first-order kinetics and a similar enantioselectivity with preferential elimination of (−)-(*S*)-FA. The $T_{1/2}$ of (−)-(*S*)-FA and (+)-(*R*)-FA was 0.92 and 3.15 h, respectively. The concentrations of (−)-*S* and (+)-(*R*)-FA were 0.60 and 30.89 mg/kg, respectively, at the time point of 12 h, and the EF was 0.02.

To clarify the mechanism of the enantioselectivity, the metabolisms of optically pure (−)-(*S*)-FE and (+)-(*R*)-FE in rabbits were studied. The (+)-(*R*)-FA was detected in rabbit plasma after injecting the single (−)-(*S*)-FE, and its concentration was significantly higher than that of its antipode at each time point (Figs. 2d and 3c). The EFs were from 0.090 to 0.019 during assays. However, the (−)-(*S*)-FA was not found in plasma after administration of (+)-(*R*)-FE (Figs. 2e and 3d). The results clearly indicated that there was chiral conversion from (−)-(*S*)-FE or (−)-(*S*)-FA to (+)-(*R*)-FA but no conversion from (+)-(*R*)-FE or (+)-(*R*)-FA to (−)-(*S*)-FA. Chiral conversion of FA in plasma was unidirectional and may play an important role in the enantioenrichment of (+)-(*R*)-FA. Chiral conversion of FA in plasma was likely the result of biotic interactions because the conversion rate was very fast. Stereoselective protein binding may also lead to the differences.[15,16]

Stereochemical aspects of FA toxicokinetics were evaluated after single intravenous dose. Plasma concentration–time curves of (−)-(*S*)-FA and (+)-(*R*)-FA were best described by an open three-compartment model. Compartmental toxicokinetic analysis and paired *t*-test results showed that differences between the principal toxicokinetic parameters of the two enantiomers were significant (Table 1). Plasma concentration–time curves of (−)-(*S*)-FA and (+)-(*R*)-FA after i.v. administration of *rac*-FA were also best described by an open three-compartment model, and the differences between the principal toxicokinetic parameters of the two enantiomers were significant (Table 1), indicating that distribution or elimination of FA was stereoselective. The different toxicokinetic parameters for the two enantiomers were used for elucidating the mechanisms underlying the stereoselectivity of FA metabolism in vivo.

Analytes in Rabbit Tissues

The data of the final residue in tissues such as heart, liver, kidney, lung, and bile at 12 h after i.v. administration of the *rac*-FE are shown in Table 2. In accord with that in plasma,

TABLE 1. Toxicokinetic parameters of FA enantiomers after i.v. administration with *rac*-FE and *rac*-FA of 30 mg/kg body weight in rabbit

Toxicokinetic Parameters	Administration with *rac*-FE		Administration with *rac*-FA	
	(−)-(*S*)-FA	(+)-(*R*)-FA	(−)-(*S*)-FA	(+)-(*R*)-FA
$t_{1/2\alpha}$ (h)	0.060	0.033	0.126	1.576
$t_{1/2\beta}$ (h)	0.883	3.080	0.734	9.342
$t_{1/2\gamma}$ (h)	69.315	69.315	36.015	9.345
*V*1 (L/kg)	0.215	0.197	0.123	0.093
CL (L/h/kg)	0.773	0.023	0.352	0.012
$t_{1/2z}$ (h)	11.929	6.216	7.555	6.517
AUC (0-*t*) (mg/L*h)	10.230	436.083	23.851	807.424
AUC (0-∞) (mg/L*h)	15.418	580.813	28.674	1097.899
MRT (0-*t*) (h)	2.642	4.498	2.371	4.292
MRT (0-∞) (h)	11.538	9.505	7.197	8.819

parent compound was not detected in the tissues except for the lung. (−)-(*S*)-FA degraded faster than its antipode in the heart, lung, liver, kidney, and bile, and both enantiomers were undetected in brain, fat, spleen, and muscle. In particular, in the lung, the concentration of (−)-(*S*)-FE and (+)-(*R*)-FE was 189.8 and 192.8 μg/g, respectively, and there was no obvious stereoselectivity with EF of 0.496; the concentration of the (−)-(*S*)-FA was a little lower than that of the (+)-(*R*)-FA with EFs of 0.415. Typical chromatograms for analytes in heart, liver, kidney, and lung tissues after i.v. administration of the *rac*-FE are shown in Figure 2. The (+)-enantiomer concentrations were in the following order at 12 h: kidney > bile > heart > lung > liver. For the (−)-enantiomer, the order was as follows: lung > kidney > bile > heart > lung > liver. These results indicated that there was substantial stereoselectivity on degradation or distribution of FA enantiomers in rabbit.

After i.v. administration of the *rac*-FA, correlative data of the final residue at 12 h are shown in Table 2. The results of administration with the *rac*-FA were similar to those of administration with the *rac*-FE. (−)-(*S*)-FA was observed to have significantly lower concentration ($P < 0.01$) than its antipode in the heart, lung, liver, kidney, and bile, and both enantiomers were undetected in brain, fat, spleen, and muscle. The (+)-enantiomer concentrations were in the following order: kidney > bile > heart > lung > liver, whereas the (−)-enantiomer as followed: lung > kidney > bile > heart > lung > liver. These results indicated that there was substantial stereoselectivity on degradation or distribution of FA enantiomers in rabbits.

The (+)-(*R*)-FA could be detected in rabbit heart, liver, kidney, bile, and lung after injecting the single (−)-(*S*)-FE, but (−)-(*S*)-FA nearly disappeared. However, the (−)-(*S*)-FA was not found in these tissues after administration of (+)-(*R*)-FE, whereas (+)-(*R*)-FA was still detected. The results showed that FA underwent a unidirectional metabolic inversion of the (−)-(*S*)-FA to its antipode with no other change in vivo.

There were several possible factors involved in the stereoselective behaviors of FA enantiomers in vivo. The first factor was chiral inversion of the (−)-(*S*)-FA in plasma. The second factor was likely stereoselective distribution of (−)-(*S*)- and (+)-(*R*)-FA in tissues. In this study, the concentration of FE was very high in the lung because of lung first-pass effect, and the stereoselective distribution may be happened when FE was transported to the other tissues.[16] Stereoselective metabolism and excretion would also result in stereoselective behavior of the chiral chemicals in animals.

In Vitro Kinetic Degradation in Plasma and Liver Microsomes

Concentration–time curves of (−)-(*S*)- and (+)-(*R*)-FE after incubation of *rac*-FE at 30 μM in rabbit plasma are shown in Figure 4. The biotransformation of FE to FA was stereoselective in favor of the (−)-(*S*)-FE, but at a much slower rate. Furthermore, the enantiospecific disappearance of the (−)-(*S*)-FE was certified indirectly by the preferential generation of (−)-(*S*)-FA. The $t_{1/2}$ of (−)-(*S*)- and (+)-(*R*)-FE was 64.8 and 91.2 min, respectively, and the EFs decreased with time from 0.492 to 0.409. At the same time, the EFs of the metabolite FA decreased with time from 0.864 to 0.561. A *t*-test between the EFs of FE and EF = 0.5 yielded a *P* value of 0.002. Enantioselectivity existed in the degradation of FE. In contrast to the result of incubation of *rac*-FE, the elimination of (−)-(*S*)- and (+)-(*R*)-FA after incubation of *rac*-FA at 30 μM in plasma was very slow with EFs from 0.500 to 0.509. Further analysis using a paired *t*-test indicated that there was no statistical significance ($P = 0.117$). There was no enantioselectivity in the degradation of FA. These data may be important to elucidate that the difference between two FE enantiomers was attributed to the stereoselective elimination of FE in plasma. Results of the incubation with single (−)-(*S*)- and (+)-(*R*)-FE at 30 μM in plasma indicated that there was no chiral conversion from (−)-(*S*)-FE or (−)-(*S*)-FA to

TABLE 2. Concentrations and EFs in plasma and tissues at 12 h following i.v. administration with *rac*-FE and *rac*-FA at 30 mg/kg body weight in rabbit[a]

Plasma and tissues	i.v. administration with FE			i.v. administration with FA		
	(−)-(*S*)-FA (mg/kg)	(+)-(*R*)-FA (mg/kg)	EF	(−)-(*S*)-FA (mg/kg)	(+)-(*R*)-FA (mg/kg)	EF
Plasma	ND[b]	18.92 ± 3.71		0.60 ±0.03	30.89 ± 4.27	0.019 ± 0.004
Kidney	1.68 ± 0.21	81.16 ± 9 10	0.020 ± 0.005	0 81 ± 0.08	84.30 ± 8 49	0.010 ± 0.001
Bile	1.26 ± 0.12	35.65 ± 5.39	0.034 ± 0.012	1.97 ± 0.33	44.27 ± 4.22	0.043 ± 0.011
Lung	5.47 ± 0.16	7.72 ± 0.95	0.415 ± 0.023	9.94± 1.10	18.31 ± 4.06	0.352 ± 0.019
Heart	0.20 ± 0.06	4.95 ± 0.69	0.039 ± 0.012	0.89 ± 0.11	7.91 + 1.29	0.101 ± 0.008
Liver	0.31 ± 0.02	2 77 ± 0.57	0.101 ± 0.012	0 88 ± 0.56	6.62 + 0.77	0.117 ± 0.010

[a]Values represent the mean ± SD ($n = 6$).
[b]Not detected.

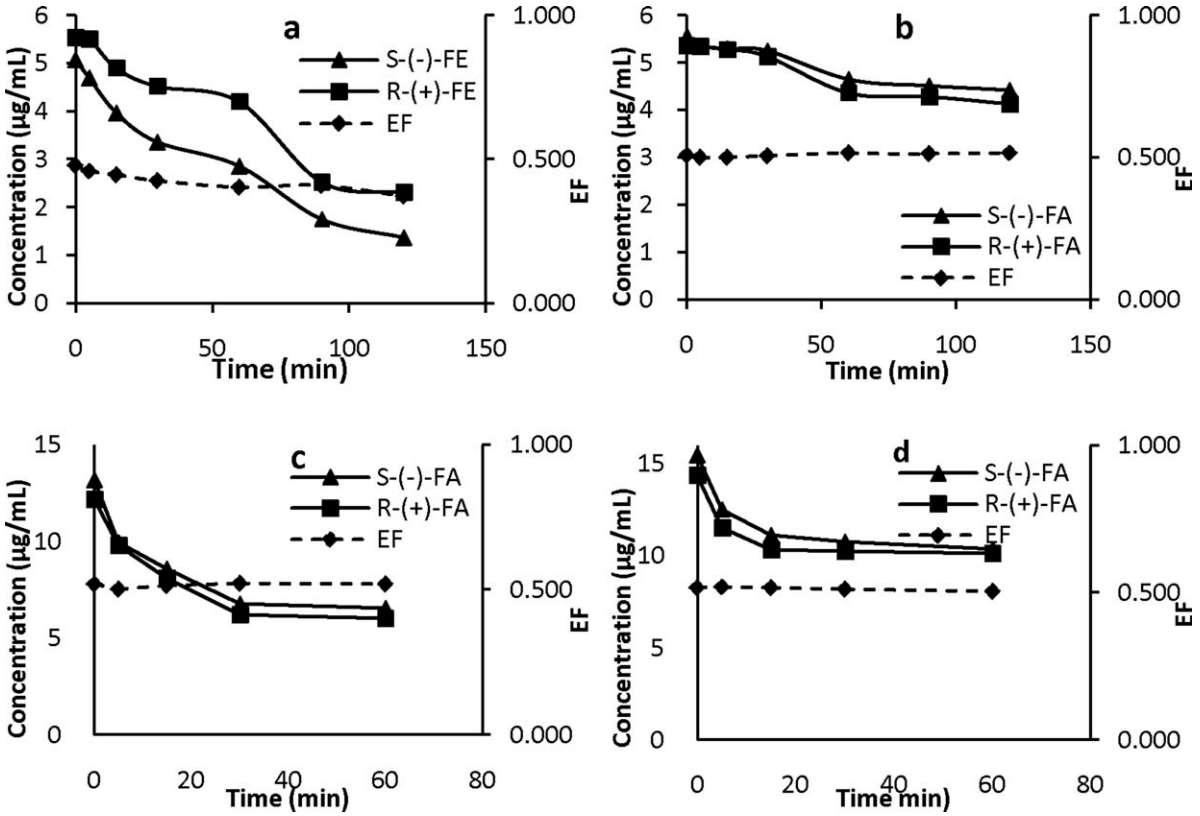

Fig. 4. Concentration–time curves of FE enantiomers or FA enantiomers with incubation of (**a**) *rac*-FE (10 μg/ml) and (**b**) *rac*-FA (10 μg/ml) in 10% plasma, (**c**) *rac*-FE (30 μM) and (**d**) *rac*-FA (30 μM) in liver microsomes.

(+)-(*R*)-FA and vice versa. This suggested that plasma was not the major site for the chiral conversion.

The possible metabolisms of FE and FA in liver were examined by the degradation of *rac*-FE, *rac*-FA, (−)-(*S*)-FE, and (+)-(*R*)-FE in liver microsomes in vitro. The metabolism of *rac*-FE at 30 μM in liver microsomes showed that (−)-(*S*)- and (+)-(*R*)-FE were metabolized very quickly to FA and became undetectable after incubation. The concentrations of the metabolite FA enantiomers were approximately equal at the period of incubation with EFs from 0.504 to 0.523, revealing that the degradation of FA in liver microsomes was nonenantioselective (Fig. 4). The metabolism of *rac*-FA in hepatic microsomes was also investigated at 30 μM. There was not significant enantiomer enrichment between the dispositions of the (−)-(*S*)- and (+)-(*R*)-FA with EFs from 0.506 to 0.521, also suggesting that the metabolism of FA in liver microsomes was nonenantioselective (Fig. 4). The observation was similar to the nonstereoselective FA elimination in plasma in vitro, but not consistent with the stereoselective toxicokinetics of FA in vivo. Such nonenantioselective metabolism could not account for the dramatic difference observed in rabbit liver and revealed that the metabolism in liver would not have led to the observed enantioenrichment of (+)-(*R*)-FA in liver tissues. Chiral inversion of FA enantiomers was not observed in microsomes with the incubation with single (−)-(*S*)- and (+)-(*R*)-FE at 30 μM in rabbit liver microsomes.

Enzyme Kinetic Analysis of Liver Microsomes

An in vitro enzyme kinetics study was conducted to investigate the stereoselective inhibition of microsomal enzymes by FE and FA. Metabolic rate constants (Table 3) of FE were calculated using linear regression, and Michaelis–Menten plot is shown in Figure 5a. The parameters did not differ significantly between the enantiomers, and the inhibition of microsomal enzymes was nonstereoselective. For *rac*-FA, metabolic rate constants (Table 3) were calculated using nonlinear regression, and Michaelis–Menten plot is shown in Figure 5b. The two enantiomers had identical enzyme kinetic characteristics, and no significant stereoselectivity was found in the inhibition by FA.

(−)-(*S*)-FA degraded faster than its antipode in the plasma, heart, lung, liver, kidney, and bile in vivo, while there was nonstereoselectivity in 10% plasma and microsomes incubation in vitro except that (−)-(*S*)-FE was stereoselectively eliminated. The fact that in vivo and in vitro results revealed significant differences was observed in previous studies.[17–20] Several reasons have been offered to explain the in vitro and in vivo discrepancy. It may be due to enantioselectivity in some of these downstream processes, and there was no

TABLE 3. Metabolic rate constants of FE and FA in rabbit liver microsomes[a]

Substrate	V_{max} (μmol /min/mg protein)	K_m (μM)	CL_{int} (ml/min/mg protein)
(−)-(*S*)FE	1674.3 ± 628.9	51409.8 ± 8867.9	32.6 ± 9.8
(+)-(*R*)-FE	1021.1 ± 709.1	31431.4 ± 9276.6	32.5 ± 92
(−)-(*S*)-FA	8.6 ± 1.3	225.3 ± 70.0	38.4 ± 4.9
(+)-(*R*)-FA	7.9 ± 1.0	175.2 ± 50.1	45.1 ± 10.9

[a]Values represent the mean ± SD (n = 6).

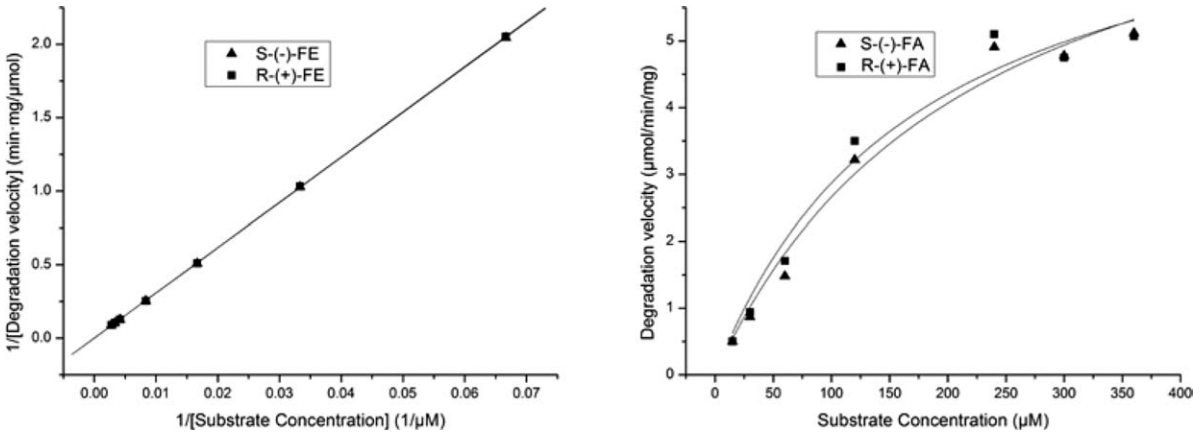

Fig. 5. Degradation rate of (−)-(*S*)-FE and (+)-(*R*)-FE (left), (−)-(*S*)-FA and (+)-(*R*)-FA (right) in rabbit liver microsomes after 30-min incubation of *rac*-FE and *rac*-FA.

significant metabolism or enantioenrichment induced by the initial plasma attack. Alternatively, selective uptake and transport across tissues or selective protein binding may also be responsible for the enantiomer enrichment of FA.[21,22] However, it should be noted that a variety of other potentially enantioselective enzyme activities may exist in vivo in rabbits, which may also act upon FA enantioselectively.

CONCLUSIONS

The chiral HPLC method described in this investigation was validated for the study of the stereoselective metabolism of the FE and FA enantiomers in rabbits. The in vivo study showed that the degradation and the toxicokinetic behavior of FA were stereoselective in rabbits, and (−)-(*S*)-enantiomer was preferentially eliminated in plasma and tissues compared with its antipode. The in vitro investigation of the stereoselective metabolisms of the enantiomers in plasma and liver microsomes demonstrated that there was no significant stereoselectivity was noted in the metabolism except the stereoselective degradation of the (−)-(*S*)-FE by plasma. The data for the enantioselective behaviors in the degradation of the enantiomers may have some implication for the environmental and ecological risk assessment for chiral pesticides or their chiral metabolites.

LITERATURE CITED

1. Bieringer HH, Hörlein G, Langelueddeke P, Handte R. HOE 33171—a new selective herbicide for the control of annual and perennial warm climate grass weeds in broadleaf crops. Proc Brit Crop Prot Conf Weeds 1982;1:11–17.
2. Kurihara N, Miyamoto J, Paulson GD, Zeeh B, Skidmore MW, Hollingworth RM, Kuiper HA. Chirality in synthetic agrochemicals: bioactivity and safety consideration. Pure Appl Chem 1997;69:2007–2025.
3. Yang D, Li X, Tao S, Wang Y, Cheng Y, Zhang D, Yu L. Enantioselective behavior of α-HCH in mouse and quail tissues. Environ Sci Technol 2010;44:1854–1859.
4. Wang Q, Qiu J, Zhu W, Jia G, Li J, Bi C, Zhou Z. Stereoselective degradation kinetics of theta-cypermethrin in rats. Environ Sci Technol 2006;40:721–726.
5. Zhu W, Qiu J, Dang Z, Lv C, Jia G, Li L, Zhou Z. Stereoselective degradation kinetics of tebuconazole in rabbits. Chirality 2007;19:141–147.
6. Warner NN, Martin JW, Wong CS. Chiral polychlorinated biphenyls are biotransformed enantioselectively by mammalian cytochrome P-450 isozymes to form hydroxylated metabolites. Environ Sci Technol 2009;43:114–121.
7. Lehmler H-J, Robertson LW, Garrison AW, Kodavanti PRS. Effects of PCB 84 enantiomers on [^{3}H]-phorbol ester binding in rat cerebellar granule cells and $^{45}Ca^{2+}$-uptake in rat cerebellum. Toxicol Lett 2005; 156:391–400.
8. Hoekstra PF, Burnison BK, Neheli T, Muir DCG. Enantiomer-specific activity of o,p′-DDT with the human estrogen receptor. Toxicol Lett 2001;125:75–81.
9. Wong CS. Environmental fate processes and biochemical transformations of chiral emerging organic pollutants. Anal Bioanal Chem 2006;386:544–558.
10. Buser HR, Müller MD, Rappe C. Enantioselective determination of chlordane components using chiral high-resolution gas chromatography-mass spectrometry with application to environmental samples. Environ Sci Technol 1992;26:1533–1540.
11. Larsson C, Ellerichmann T, Hühnerfuss H, Bergman Å. Chiral PCB methyl sulfones in rat tissues after exposure to technical PCBs. Environ Sci Technol 2002;36:2833–2838.
12. Zhang P, Zhu W, Dang Z, Shen Z, Xu X, Huang L, Zhou Z. Stereoselective metabolism of benalaxyl in liver microsomes from rat and rabbit. Chirality 2011;23:93–98.
13. Fang L, Bykowski-Jurkiewicz C, Sarver J, Erhardt PW. Determination of esmolol and metabolite enantiomers within human plasma using chiral column chromatography. J Chromatogr B 2010;878:2449–2452.
14. Anand SS, Bruckner JV, Haines WT, Muralidhara S, Fisher JW, Padilla S. Characterization of deltamethrin metabolism by rat plasma and liver microsomes. Toxicol Appl Pharm 2006;212:156–166.
15. Kunze KL, Nelson WL, Kharasch ED, Thummel KE, Isoherranen N. Stereochemical aspects of Itraconazole metabolism *in vitro* and *in vivo*. Drug Metab Dispos 2006;34:583–590.
16. Hanada K, Ikemi Y, Kukita K, Mihara K, Ogata H. Stereoselective first-pass metabolism of Verapamil in the small intestine and liver in rats. Drug Metab Dispos 2008;36:2037–2042.
17. Yamano K, Yamamoto K, Katashima M, Kotak H, Takedomi S, Matsuo H, Ohtani H, Sawada Y, Iga T. Prediction of midazolam-CYP3A inhibitors interaction in the human liver from in vivo/in vitro absorption, distribution and metabolism data. Drug Metab Dispos 2001;29:443–452.
18. Wing KD, Glickman AH, Casida JE. Oxidative bioactivation of *S*-alkyl phosphorothiolate pesticides: stereospecificity of profenofos insecticide activation. Science 1983;219:63–65.
19. Mohri K, Okada K, Benet LZ. Stereoselective taurine conjugation of (*R*)-Benoxaprofen enantiomer in rats *in vivo* and *in vitro* studies using rat hepatic mitochondria and microsomes. Pharm Res 2005;22:79–85.
20. Nillos MG, Chajkowski S, Rimoldi JM, Gan J, Lavado R, Schlenk D. Stereoselective biotransformation of permethrin to estrogenic metabolites in fish. Chem Res Toxicol 2010;23:1568–1575.
21. Covaci A, Gheorghe A, Schepen P. Distribution of organochlorine pesticides, polychlorinated biphenyls and α-HCH enantiomers in pork tissues. Chemosphere 2004;56:757–776.
22. Ulrich EM, Willett K, Caperell-Grant A, Bigsby RM, Hites RA. Understanding enantioselective processes: a laboratory rat model for R-hexachlorocyclohexane accumulation. Environ Sci Technol 2001;35: 1604–1609.